ANALYTICAL SCIENCES JULY 2017, VOL. 33

Determination of the Electrostatic Potential of Oil-in-Water Emulsion Droplets by Combined Use of Two Membrane Potential-Sensitive Dyes

Tomoya IWATA,* Hirohisa NAGATANI, and Toshiyuki OSAKAI*†**

**Department of Chemistry, Graduate School of Science, Kobe University, Nada, Kobe 657–8501, Japan*
***Faculty of Chemistry, Institute of Science and Engineering, Kanazawa University, Kakuma, Kanazawa 920–1192, Japan*

The fluorescence behaviors of potential-sensitive dyes including anionic $DiBAC_4(3)$ (denoted by dye **A**), $DiSBAC_2(3)$ (dye **B**), and zwitterionic di-4-ANEPPS (dye **C**) were studied in oil-in-water (O/W) emulsions. In this study, the equilibrium Galvani potential difference ($\Delta_O^W\phi_{eq}$) of the O/W-emulsion droplets was controlled by changing the ratio of the concentrations of electrolytes added to the O (=1,2-dichloroethane) and W phases. When using an adequate combination of the dyes, *i.e.*, **B** and **C**, we could observe that the ratio of their fluorescence peak intensities was changed from 1.08 to 1.38, depending on the change of ($\Delta_O^W\phi_{eq}$ from 26 to 73 mV. It is desirable to apply this method to study the potential-dependent ion or electron-transfer reactions occurring at vesicles or liposomes, and also to biomembranes.

Keywords Membrane potential-sensitive dyes, O/W emulsion, Galvani potential difference, fluorescence spectroscopy

(Received January 30, 2017; Accepted March 10, 2017; Published July 10, 2017)

Introduction

The electrostatic or Galvani potential difference across a biomembrane is a key factor for controlling electron and/or ion transfer across the membrane in neurotransmission systems as well as respiratory and photosynthetic electron-transport systems.[1] So far, the microelectrode technique[2] has been used to determine membrane potentials for relatively large cells (*e.g.*, squid axon,[3] Xenopus oocyte,[4] *etc.*). The patch clamp technique[5] with a glass micropipette was also applied to measure the membrane potential of relatively small cells of 5 – 10 μm.[6] However, these microelectrode techniques are difficult to apply to neuron cells with fine structures or complex multicellular preparations. To overcome these difficulties, potential-sensitive dyes (PSDs) have been developed, which change their fluorescent intensity and/or wavelength in response to changes in the biomembrane potential.[7-9] The dyes have been used for optical monitoring of the activities for various neural tissues, which are accompanied by changes of the membrane potential.[10-15] Usually, however, the potential change is only monitored through changes in the fluorescent intensity. It should be noted that PSDs generally exhibit a very slight change in the fluorescent wavelength (just a few nm, as described by Loew).[9] Nevertheless, Loew's group[16] developed an integrated method in which the ratio of fluorescence excited at two different wavelengths was linearly dependent on the membrane potential for HeLa cells. In the measurement, a zwitterionic PSD, 1-(3-sulfonatopropyl)-4-[β-{2-(di-*N*-butylamino)-6-naphthyl}-vinyl]pyridinium betaine (di-4-ANEPPS), was employed as an internal probe.

On the other hand, we have utilized a spectroelectrochemical method called potential-modulated fluorescence (PMF) spectroscopy[17,18] to study the fluorescence behavior of some different PSDs at the polarized oil (O)|water (W) interface used as a biomembrane model.[19-22] Then, the potential-dependent fluorescence behavior of the PSDs could be elucidated in terms of relatively slow processes, such as reorientation or adsorption/desorption reactions at the interface. In a recent study,[21] it was shown that two anionic PSDs, bis-(1,3-dibutylbarbituric acid) trimethine oxonol ($DiBAC_4(3)$) and bis-(1,3-diethylthiobarbituric acid)trimethine oxonol ($DiSBAC_2(3)$), gave well-defined PMF signals due to adsorption/desorption at the 1,2-dichloroethane (DCE)|W interface. The PMF signals were separated by about 100 mV. We then attempted a combined use of the two dyes for determining the Galvani potential difference ($\Delta_O^W\phi_{eq}$) across the DCE|W interface. When the dyes were added at appropriate concentrations to the W phase, distinctly different PMF spectra were obtained at different interfacial potentials. The ratio of the PMF signal intensities at the fluorescence maximum wavelengths for the respective dyes showed a clear dependence on $\Delta_O^W\phi_{eq}$. These results suggested the potential utility of the combined use of two dyes for determining the electrostatic potential of biological cells and their models, including liposomes, oil-in-water (O/W) emulsions, *etc*. In this study we have tried to use two PSDs for determining the electrostatic potential for O/W-emulsion droplets.

† To whom correspondence should be addressed.
E-mail: osakai@kobe-u.ac.jp

Experimental

$DiBAC_4(3)$ (denoted hereafter by dye **A**), $DiSBAC_2(3)$ (dye **B**), and di-4-ANEPPS (dye **C**) were purchased from Takara Bio, AnaSpec, and Wako Pure Chemical Industries, respectively. For the experiments using O/W emulsion, stock DCE solutions of dye **A** {3.98×10^{-5} M (= mol dm^{-3})}, dye **B** (2.94×10^{-4} M), and dye **C** (3.70×10^{-5} M) were prepared and stored in a refrigerator.

Tetrapropylammonium chloride (TPrACl; Sigma-Aldrich), tetraethylammonium chloride (TEACl; Tokyo Chemical Industry), sodium dodecyl sulfate (SDS; Sigma-Aldrich), and DCE (for HPLC; Wako Pure Chemical Industries) were purchased and used as received. Tetrapropylammonium and tetraethylammonium salts of tetrakis(4-chlorophenyl)borate (TPrATClPB and TEATClPB) were prepared by equimolar mixing of an ethanol solution of TPrACl or TEACl with an ethanol solution of potassium tetrakis(4-chlorophenyl)borate (Tokyo Chemical Industry); the resultant crude crystals were washed five times with purified water, and then recrystallized from 1:1 (v/v) acetone–ethanol. All other reagents were of the analytical grade and used as received.

By referring to previous papers,[23–26] O/W emulsions were prepared as follows: 2 mL of DCE containing 5 mM TPrATClPB (or TEATClPB) and a certain concentration(s) of one or two PSDs and 50 mL of W containing 10 mM SDS and different concentrations of TPrACl (or TEACl) were added to a 100-mL glass bottle; the mixture was then homogenized by sonication at 21 kHz for 60 s using an ultrasonic homogenizer (VIOLAMO, SONICSTAR85; the output was set at 70% of the maximum level). The droplets of the O/W emulsions prepared were observed with a digital microscope (KEYENCE, VH-5500); the size of most droplets was about 2 μm, though much larger droplets were occasionally observed, as exemplified in Fig. S1 (Supporting Information).

Since the PSDs used in this study were all hydrophobic, they seem to remain mostly in the O-phase side, but a certain amount would be adsorbed at the surfaces of O/W-emulsion droplets depending on the electrostatic potential. The fluorescence of O/W emulsions containing one or two PSDs was measured by a fluorescence spectrometer (Shimadzu, RF-5300PC) using an excitation wavelength of 473 nm. The measurements were carried out at room temperature in a quartz cuvette with a path length of 1 cm.

Results and Discussion

Estimation of the electrostatic potential of O/W-emulsion droplets

In this study the equilibrium Galvani potential difference ($\Delta_O^W\phi_{eq}$) of O/W-emulsion droplets was estimated by using a theory[27–29] proposed for the estimation of $\Delta_O^W\phi_{eq}$ for O|W interfaces. In applying the theory, it has been assumed that each ion (i) in the O|W system is distributed in equilibrium between the O and W phases and that, for simplicity, no ion pair is formed in either phase. The latter assumption may be somewhat inaccurate for the DCE phase, but DCE has a moderately high dielectric constant ($\varepsilon_r = 10.37$[30] at 25°C). In this theory we define the following functions, ξ_i^W and ξ_i^O:

$$\xi_i^W = \frac{z_i c_i^{0,W}}{1 + r\exp\left[\frac{z_i F}{RT}(\Delta_O^W\phi - \Delta_O^W\phi_i^\circ)\right]}, \quad (1)$$

Table 1 Standard ion-transfer potentials of $TPrA^+$, TEA^+, Na^+, Cl^-, DS^-, and $TClPB^-$ at the DCE|W interface (25°C)

Ion	$\Delta_O^W\phi_i^\circ$/V
$TPrA^+$	–0.09[a]
TEA^+	+0.02[a]
Na^+	+0.59[a]
Cl^-	–0.53[a]
DS^-	+0.08[b]
$TClPB^-$	+0.59[c]

a. From Ref. 31.
b. From Ref. 32.
c. Determined by ion-transfer voltammetry.

$$\xi_i^O = \frac{r z_i c_i^{0,O}}{1 + r\exp\left[\frac{z_i F}{RT}(\Delta_O^W\phi - \Delta_O^W\phi_i^\circ)\right]}, \quad (2)$$

where z_i and $\Delta_O^W\phi_i^\circ$ are the charge number (including the sign) and the standard ion-transfer potential for ion i, respectively; $c_i^{0,\alpha}$ (α = W or O) is the initial concentration of ion i added to the W or O phase; F, R, and T have their usual meanings; and r is the volume ratio of the O and W phases, being given by

$$r = \frac{v^O}{v^W}. \quad (3)$$

In the present experiments, r = (2.0 mL/50 mL) = 0.040, since the mutual solubility of DCE and W is less than 1 wt%. If the total sum of ξ_i^W and ξ_i^O for all ions given by

$$\xi_{total} = \sum_i \xi_i^W + \sum_i \xi_i^O \quad (4)$$

is 0, then $\Delta_O^W\phi$ in Eqs. (1) and (2) corresponds to the equilibrium potential difference, *i.e.*, $\Delta_O^W\phi_{eq}$.

The values of $\Delta_O^W\phi_i^\circ$ required for the calculation of $\Delta_O^W\phi_{eq}$ have been obtained from the literature,[31,32] except for $TClPB^-$ (see Table 1). The $\Delta_O^W\phi_i^\circ$ of $TClPB^-$ was obtained by ion-transfer voltammetry with the polarized DCE|W interface. In a similar manner to that reported previously,[33] the value of $\Delta_O^W\phi_{TClPB^-}^\circ$ (= +0.59 V) was estimated from the positive-current final rise of the cyclic voltammogram by referring to that of the tetraphenylborate ion (*i.e.*, $\Delta_O^W\phi_{TPB^-}^\circ$ = +0.364 V).[34] It should be noted here that the influence of PSDs for estimating $\Delta_O^W\phi_{eq}$ should be negligibly small, because their initial concentration was very low, *i.e.*, in the order of several tens of μM in DCE.

Throughout the present experiments, SDS was initially added to the W phase at a sufficient concentration (10 mM) for the stable formation of O/W emulsions. Accordingly, it is considered that a certain amount of SDS is adsorbed upon saturation at the surfaces of O/W-emulsion droplets, so that the total amount of DS^- and Na^+ distributed to both phases should be decreased to a certain extent. We then estimated the amount of SDS adsorbed at the droplet surfaces from the averaged size of the droplets (2 μm, *vide supra*) and the area occupied per molecule of SDS (45 – 65 Å^2 as reported for various hydrocarbon|water interfaces).[35] The estimation showed that only 3.1 – 4.4% of SDS is adsorbed at the droplet surfaces. This amount does not very much influence the estimation of $\Delta_O^W\phi_{eq}$ in the present system (the error is within several millivolts). In the following estimation, however, we have assumed that 5% of SDS (*i.e.*, DS^- and Na^+) is adsorbed at the droplet surfaces, with the remaining 95% being distributed between the O and W phases.

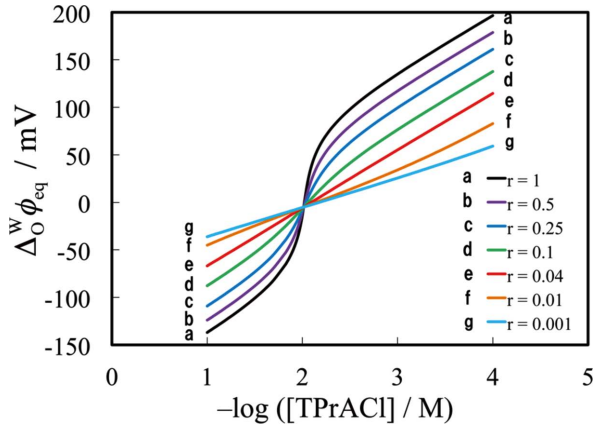

Fig. 1 Change of $\Delta_O^W\phi_{eq}$ with –log([TPrACl]/M) for the $TPrA^+$ system with [TPrATClPB] = 5 mM and [SDS] = 10 mM. r = (a) 1, (b) 0.5, (c) 0.25, (d) 0.1, (e) 0.04, (f) 0.01, (g) 0.001. It is assumed that 5% of SDS is adsorbed at the O-droplet surfaces.

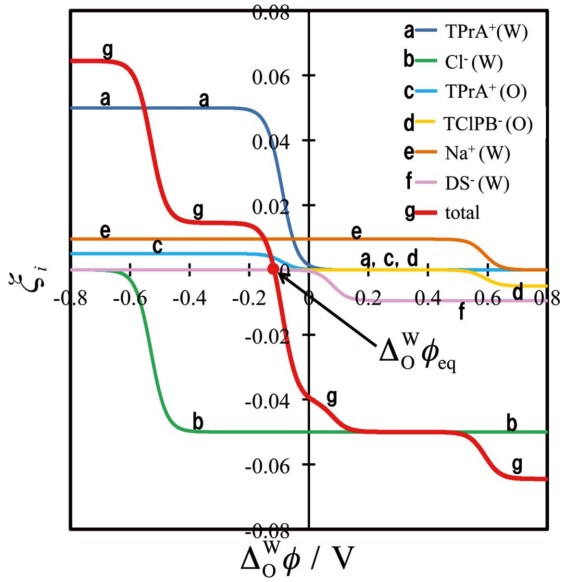

Fig. 2 Dependences of ξ_i^W or ξ_i^O on $\Delta_O^W\phi$ in the $TPrA^+$ system (with r = 1). [TPrACl] = 50 mM; [TPrATClPB] = 5 mM; [SDS] = 10 mM (it is assumed that 5% of SDS is adsorbed at the O-droplet surfaces). i = (a) $TPrA^+$ (W), (b) Cl^- (W), (c) $TPrA^+$ (O), (d) $TClPB^-$ (O), (e) Na^+ (W), (f) DS^- (W), (g) for all ions, *i.e.*, ξ_{total} being given by Eq. (4).

Figure 1 shows the change of $\Delta_O^W\phi_{eq}$ with –log([TPrACl]/M) for the $TPrA^+$ system with [TPrATClPB] = 5 mM and [SDS] = 10 mM. Here, the parenthesis [ ] represents the molar concentration of an electrolyte initially added to either O or W phase; because complete dissociation has been assumed for all electrolytes in both phases, we set: $[TPrACl] = c^{0,W}_{TPrA^+} = c^{0,W}_{Cl^-}$; $[TPrATClPB] = c^{0,O}_{TPrA^+} = c^{0,O}_{TClPB^-}$; $[SDS] \times 0.95 = c^{0,W}_{DS^-} = c^{0,W}_{Na^+}$. In Fig. 1 are shown seven curves obtained for different r-values ranging from 1 to 0.001. For r = 1 – 0.1, a drastic change of $\Delta_O^W\phi_{eq}$ is observed around –log([TPrACl]/M) = 2. On the other hand, for r = 0.04 – 0.001, $\Delta_O^W\phi_{eq}$ shows a linear dependence on –log([TPrACl]/M) in the range studied. For a better understanding, we have prepared Fig. 2, in which the dependences of ξ_i^W or ξ_i^O on $\Delta_O^W\phi$ are shown for all ions involved in the $TPrA^+$ system (with r = 1; [TPrACl] = 50 mM). For example, curve a shows the potential dependence of ξ_i^W for i = $TPrA^+$; the dependence is sigmoidal, suggesting that the distribution ratio of $TPrA^+$ should be varied significantly around the potential of the inflection point corresponding to the standard ion-transfer potential of $TPrA^+$ ($\Delta_O^W\phi^\circ_{TPrA^+}$ = –0.09 V; note that here r = 1). Similarly, curve c shows the potential dependence of ξ_i^O for $TPrA^+$ added to the O phase. This curve also has an inflection point at $\Delta_O^W\phi^\circ_{TPrA^+}$. Figure 2 shows the potential dependence of ξ_i^W or ξ_i^O for the other ions, and furthermore that of ξ_{total} given by Eq. (4). The intersection point of the ξ_{total} *vs.* $\Delta_O^W\phi$ curve (curve g) and the potential axis should correspond to $\Delta_O^W\phi_{eq}$ for the system. As can be seen from Fig. 2, $\Delta_O^W\phi_{eq}$ is located around the inflection point of curves a and c (*i.e.*, $\Delta_O^W\phi^\circ_{TPrA^+}$). The values of ξ_i^W and ξ_i^O for the ions other than $TPrA^+$ exhibit no change in the potential range around $\Delta_O^W\phi_{eq}$. It has thus been suggested that the equilibrium potential for the system should be governed mostly by the Nernst distribution of $TPrA^+$. In Fig. 1, the potential dependence of $\Delta_O^W\phi_{eq}$ under these conditions is shown in the lower end part of curve a.

The situation is significantly altered by a decrease in [TPrACl]. In Figs. S2A – S2C (Supporting Information) show the potential dependences of ξ_i^W and ξ_i^O (with r = 1) obtained for three different values of [TPrACl] (= 50, 10, and 1 mM). As shown in Fig. S2C, under such conditions as [TPrACl] < [SDS], the $\xi^W_{TPrA^+}$ value, *i.e.*, the contribution of $TPrA^+$ added to the W phase becomes smaller, and in turn the contribution of DS^- becomes dominant; note that under these conditions, $\Delta_O^W\phi_{eq}$ is located close to the inflection point of the $\xi^W_{DS^-}$ *vs.* $\Delta_O^W\phi$ curve. Thus, with decreasing [TPrACl], the potential-determining ion is changed from $TPrA^+$ to DS^-. This corresponds to a drastic change of $\Delta_O^W\phi_{eq}$, being typically shown by curve a in Fig. 1.

However, as also shown in Fig. 1, there is no drastic change of $\Delta_O^W\phi_{eq}$ for smaller values of r (<0.04). This reason can be found by preparing a set of such graphs as shown in Figs. S2A – S2C for a smaller r value {=0.04; see Figs. S3A – S3C (Supporting Information)}. For smaller r values, the contribution from the ions added to the O phase, *i.e.*, ξ_i^O becomes smaller, and also the inflection points of the ξ_i^W *vs.* $\Delta_O^W\phi$ curves for $TPrA^+$ and DS^-, incidentally, give close agreements with each other (as clearly seen in Fig. S3B). As a result, $\Delta_O^W\phi_{eq}$ is mainly determined by two different ions ($TPrA^+$ and DS^-) added to the W phase. Since this situation is formally similar to that for the typical Nernst distribution of a single ion, an almost linear $\Delta_O^W\phi_{eq}$ *vs.* –log([TPrACl]/M) curve seems to be obtained (for example, see curve e in Fig. 1).

The above-mentioned calculation results for the $TPrA^+$ system are similar to those for the TEA^+ system. The obtained $\Delta_O^W\phi_{eq}$ *vs.* –log([TEACl]/M) curve is shown in Fig. S4 (Supporting Information). Thus, the $\Delta_O^W\phi_{eq}$ of the O/W-emulsion droplets can be evaluated theoretically.

Fluorescence spectra of the O/W emulsions containing dye ***A*** *or* ***B***

Figure 3 shows the fluorescence spectra of O/W emulsions containing only dye **A** (throughout this study, the reproducibility of fluorescence spectra was confirmed by at least three independent experiments). In the figure, panels A and B show the results obtained for the $TPrA^+$ and TEA^+ systems, respectively, in which [TPrACl] or [TEACl] was varied between 5.0 and 0.5 mM to change $\Delta_O^W\phi_{eq}$ of the O/W-emulsion droplets. As can be seen in the figure, with lowering the electrolyte concentration, the fluorescence peak at 519 nm monotonously decreased, though it was exceptionally increased by lowering [TPrACl] from 5 to 3 mM. Table 2 gives the theoretically estimated $\Delta_O^W\phi_{eq}$ values for five different values of [TPrACl] or [TEACl], which were used in the fluorescence measurements

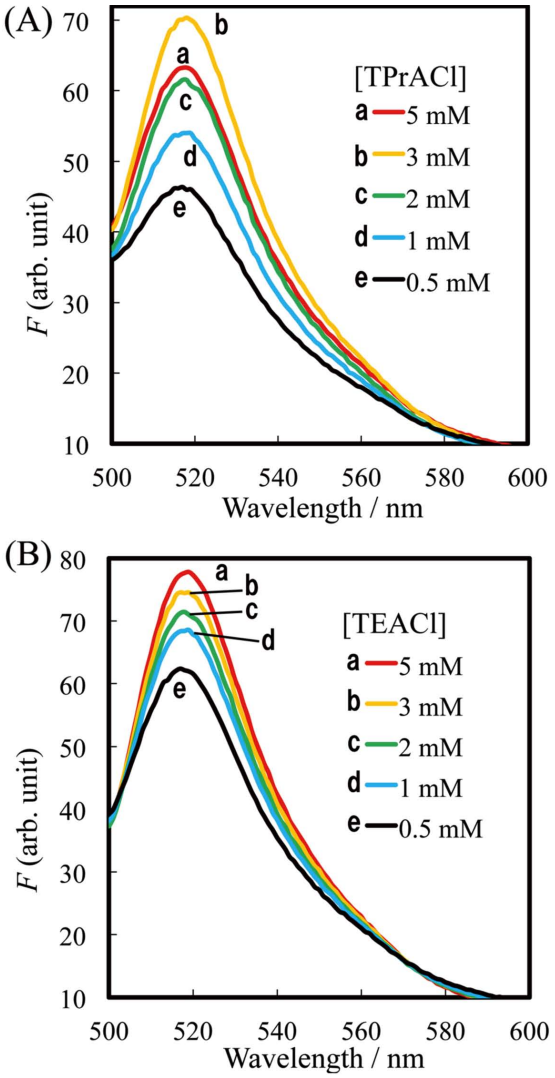

Fig. 3 Fluorescence spectra of O/W emulsions containing only dye **A** (added initially at 30 μM to DCE). [SDS] = 10 mM; r = 0.04. (A) [TPrATClPB] = 5.0 mM; [TPrACl] = 0.5, 1.0, 2.0, 3.0, and 5.0 mM. (B) [TEATClPB] = 5.0 mM; [TEACl] = 0.5, 1.0, 2.0, 3.0, and 5.0 mM. Excitation wavelength = 473 nm.

Table 2 Theoretical $\Delta_O^W\phi_{eq}$ values estimated for different concentration conditions used in the fluorescence measurements of Figs. 3 – 7 and S5 – S8 (with r = 0.04; [SDS] = 10 mM; 5% of SDS is assumed to be adsorbed at the O-droplet surfaces)

$TPrA^+$ system[a]		TEA^+ system[b]	
[TPrACl]/mM	$\Delta_O^W\phi_{eq}$/mV	[TEACl]/mM	$\Delta_O^W\phi_{eq}$/mV
5.0	13	5.0	62
3.0	26	3.0	71
2.0	37	2.0	78
1.0	55	1.0	90
0.5	73	0.5	103

a. [TPrATClPB] = 5.0 mM.
b. [TEATClPB] = 5.0 mM.

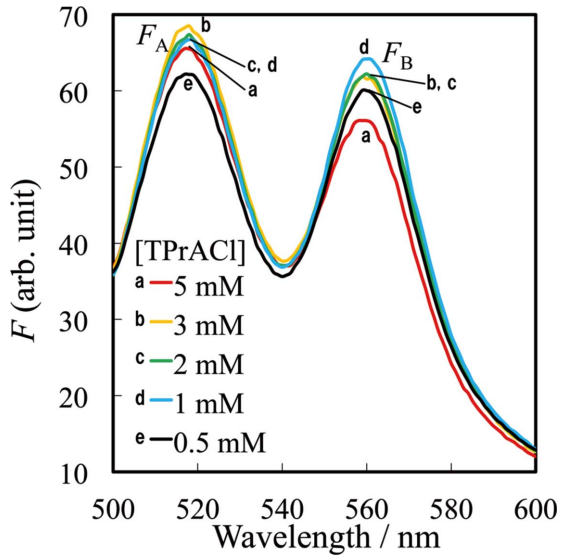

Fig. 4 Fluorescence spectra of O/W emulsions containing both dyes **A** and **B** (added initially at 30 and 20 μM, respectively, to DCE). [SDS] = 10 mM; [TPrATClPB] = 5.0 mM; [TPrACl] = 0.5, 1.0, 2.0, 3.0, and 5.0 mM; r = 0.040. Excitation wavelength = 473 nm.

shown in Fig. 3 (and others shown below in Figs. 4, 6, S5, and S8). As shown in the table, with lowering the electrolyte concentration, $\Delta_O^W\phi_{eq}$ shifts to more positive potentials. This potential change probably induced an increase in the fluorescence peak of dye **A**.

Figure S5 (Supporting Information) shows the fluorescence spectra of O/W emulsions containing only dye **B**. The experimental conditions used are the same as for dye **A** in Fig. 3. However, dye **B** showed a relatively smaller change in the intensity of the fluorescence peak at 560 nm. Also, the fluorescence intensity in the TEA^+ system (Fig. S5B) tended to *decrease* with lowering [TEACl].

As shown above, the observed behaviors of the fluorescence spectra for dyes **A** and **B** (Figs. 3 and S5) are somewhat different; however we assume that the potential-dependent fluorescence spectra could be observed for the dyes in the O/W-emulsion system.

This assumption may be supported by our previous study on the PMF responses of dyes **A** and **B** at the polarized DCE|W interface.[21] In PMF measurements, we employed a "neat" DCE|W interface (*i.e.*, without SDS), so that rigorous comparisons cannot be made with the results of the present O/W-emulsion system. However, it should be noted that dye **A** showed a significant change in the PMF signal in the range of $\Delta_O^W\phi$ corresponding to the potential range used in the present emulsion system ($\Delta_O^W\phi_{eq}$ = 13 – 103 mV; see Table 2), whereas dye **B** showed no significant change in the PMF signal in the corresponding potential range (E = 375 – 465 mV in Fig. 4 of Ref. 21). These PMF behaviors of the dyes are in harmony with the fluorescence changes shown in Figs. 3 and S5, and would strongly suggest that the changes probably come from the variation of $\Delta_O^W\phi_{eq}$ for the O/W emulsion.

In the present study, we used a higher concentration (10 mM) of SDS for the stable formation of O/W emulsions. This might result in the formation of smaller micelles (not detectable in the light microscope) and possible inclusion of the dyes in the micelles. However, it seems that fluorescence changes with variations of the electrolyte concentration occurred mainly at the O/W-emulsion droplets, whose surface potential should be controlled in the manner described above.

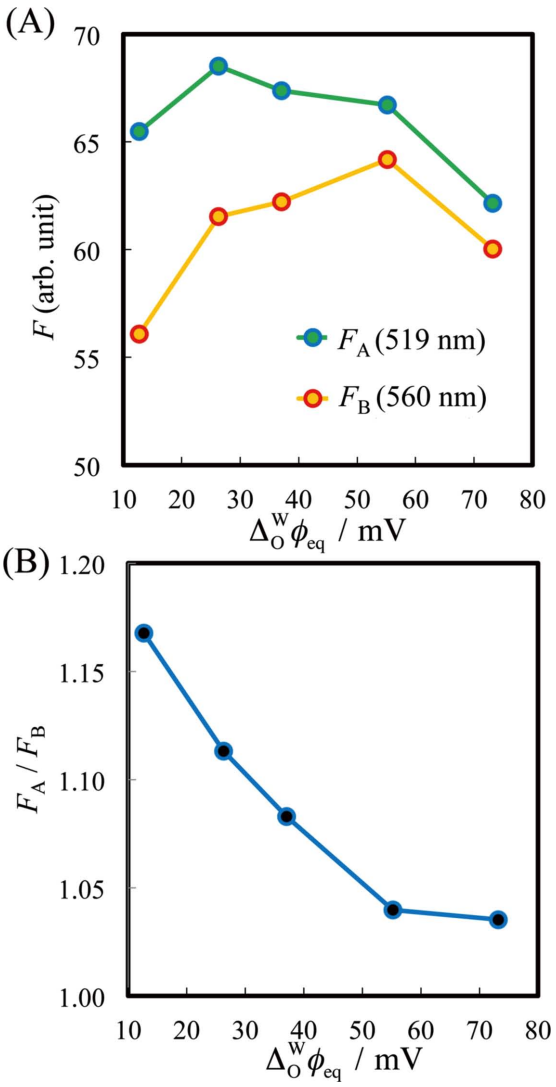

Fig. 5 (A) Intensities of the fluorescence peaks, F_A and F_B, obtained in Fig. 4 and (B) their ratio F_A/F_B, which are plotted against $\Delta_O^W\phi_{eq}$.

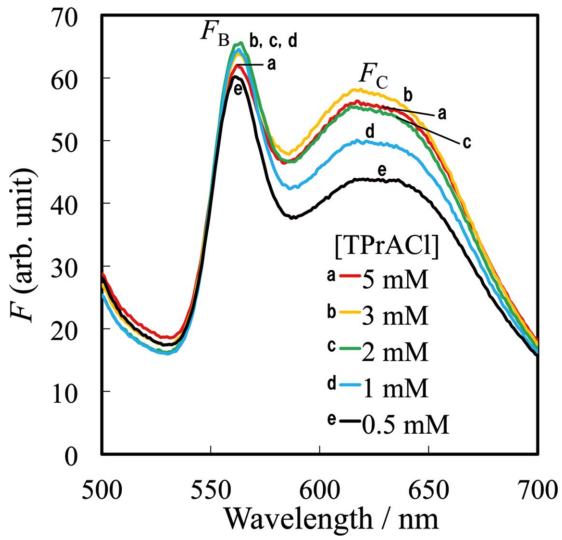

Fig. 6 Fluorescence spectra of O/W emulsions containing both dyes **B** and **C** (added initially at 25 and 40 μM, respectively, to DCE). [SDS] = 10 mM; [TPrATClPB] = 5.0 mM; [TPrACl] = 0.5, 1.0, 2.0, 3.0, and 5.0 mM; r = 0.040. Excitation wavelength = 473 nm.

*Combined use of dyes **A** and **B***

Figure 4 shows the fluorescence spectra of O/W emulsions containing both dyes **A** and **B**, in which [TPrACl] was varied between 5.0 and 0.5 mM for changing $\Delta_O^W\phi_{eq}$ in the range of 13 - 73 mV. As can be seen in the figure, the intensity of the fluorescence peak at 519 nm for dye **A** and that at 560 nm for dye **B** (being denoted by F_A and F_B, respectively) were varied somewhat, but not monotonously, as shown in Fig. 5A. The degrees of variation were not very large compared with those observed for the single use of dye **A** or **B** (Fig. 3 or S5). It should be particularly noted that the fluorescence peak for dye **A** showed a smaller change than that observed for its single use (Fig. 3). This seems to be due to quenching by dye **B** coexisting with dye **A**, *i.e.*, a non-radiative transition from the excited state of dye **A** to the ground state of neighboring dye **B**. A similar quenching effect was observed for the PMF spectra for the combined use of dyes **A** and **B**.[21] Considering this effect, we set the concentration of dye **A** at a higher value (30 μM) than that of dye **B** (20 μM) in the fluorescence measurement shown in Fig. 4. Under these conditions, the ratio F_A/F_B was measured for each [TPrACl], and then plotted against $\Delta_O^W\phi_{eq}$ in Fig. 5B; the F_A/F_B ratio showed a well-defined dependence on $\Delta_O^W\phi_{eq}$, though only a small variation was observed for the higher range of $\Delta_O^W\phi_{eq}$ (>55 mV). This result means that we could observe a potential-dependent spectral change, *i.e.*, a color-tone change, by using two dyes.

Thus, when using the $TPrA^+$ system, we obtained a satisfactory result, but when using the TEA^+ system, we could not obtain a simple F_A/F_B *vs.* $\Delta_O^W\phi_{eq}$ plot. In the TEA^+ system, the plot of interest showed a V-shaped curve, as in Fig. S6 (Supporting Information). The difference observed between the $TPrA^+$ and TEA^+ systems would be ascribed to the difference of the adsorption/desorption behaviors of the dyes in the corresponding potential ranges, though no detailed explanation is provided.

*Combined use of dyes **B** and **C***

In order to achieve a more sensitive and practical potential-dependent fluorescence spectrum, we examined combinations of dye **A** or **B** (anionic) with dye **C** (zwitterionic). For the respective combinations, we controlled $\Delta_O^W\phi_{eq}$ by changing the electrolyte concentration using the $TPrA^+$ or TEA^+ system. As the result, the combination of dyes **B** and **C** in the $TPrA^+$ system gave the most satisfactory results. The combination of these dyes in the TEA^+ system and also the combination of dyes **A** and **C** in either electrolyte system gave no satisfactory results; in these cases, the fluorescence peak ratio *vs.* $\Delta_O^W\phi_{eq}$ plot showed a V-shaped curve, as exemplified in Fig. S7 (Supporting Information).

Figure S8 (Supporting Information) shows the fluorescence spectra of O/W emulsions containing only dye **C**. In both (A) $TPrA^+$ and (B) TEA^+ systems, certain changes in the fluorescence peak intensity with the electrolyte concentrations were observed in a similar manner to those for dyes **A** and **B** (cf. Figs. 3 and S5). The spectral change observed for the combined use of **B** and **C** in the $TPrA^+$ system is shown in Fig. 6. In this case, there was no marked change in F_B at 560 nm, probably because of quenching by dye **C**. However, the fluorescence peak for dye **C** at 615 nm was considerably increased with increasing [TPrACl] from 0.5 to 3 mM. The changes of the fluorescence peak intensities for the two dyes are shown in Fig. 7A, and their ratio, F_B/F_C, is plotted against $\Delta_O^W\phi_{eq}$ in Fig. 7B. It should here

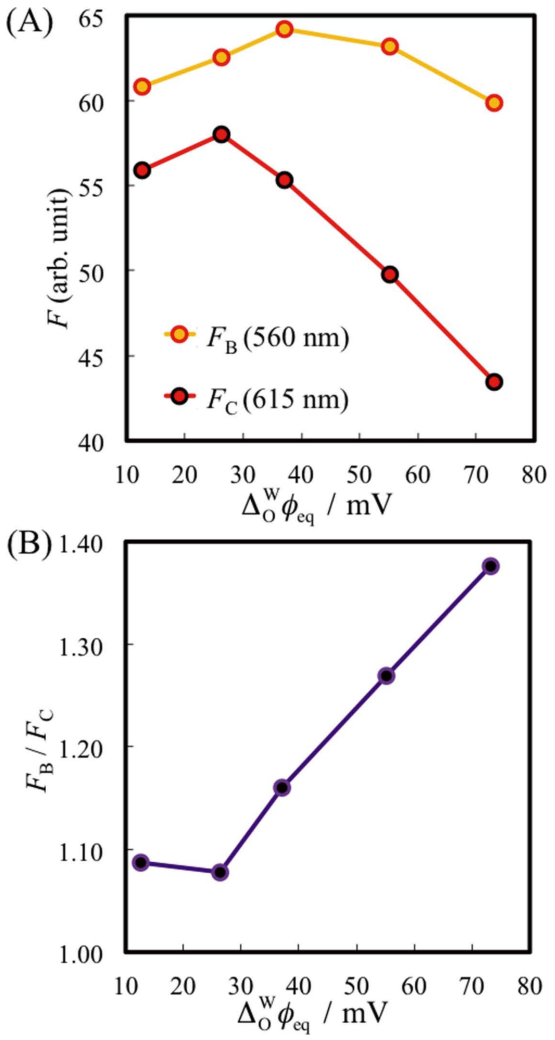

Fig. 7 (A) Intensities of the fluorescence peaks, F_B and F_C, obtained in Fig. 6 and (B) their ratio, F_B/F_C, which are plotted against $\Delta_O^W\phi_{eq}$.

be noted that the change of the F_B/F_C ratio was ranged from 1.08 to 1.38. This change was more than two-times larger than that for the F_A/F_B ratio (ranging from 1.03 to 1.16 as in Fig. 5B).

Concluding Remarks

It has been found that the fluorescence of some PSDs at O/W emulsions depends on the electrostatic potential of the O/W-emulsion droplets. For the single use of dye **A**, **B**, or **C**, the fluorescence peak changes, mainly in the intensity, by changing the equilibrium Galvani potential difference ($\Delta_O^W\phi_{eq}$) of the O/W-emulsion droplets. When using an adequate combination of two dyes, a well-defined change in the spectral shape can be obtained; for example, when using dyes **B** and **C**, the ratio of the fluorescence peak intensities for the dyes changes from 1.08 to 1.38, depending on the change of $\Delta_O^W\phi_{eq}$ in the range from 26 to 73 mV. These findings would suggest a possible application of PSDs to the study of potential-dependent ion or electron transfer reactions occurring at O/W-emulsion droplets. In addition, it is desirable to apply the presently developed method (*i.e.*, the combined use of two PSDs) to vesicles or liposomes, and also to biomembranes.

Acknowledgements

The authors are grateful to Prof. Jingyuan Chen (Fukui University) for her helpful advice for preparing O/W emulsions. The authors also thank Mr. Hiroyuki Okawa and Prof. Minoru Mizuhata (Kobe University) for their help in photomicroscopic observation of O/W-emulsion droplets.

Supporting Information

Optical micrograph of the O/W emulsion (Fig. S1), dependences of ξ_i^W and ξ_i^O on $\Delta_O^W\phi$ (Figs. S2 and S3), change of $\Delta_O^W\phi_{eq}$ with –log([TEACl]/M) (Fig. S4), and additional fluorescence data (Figs. S5 – S8). This material is available free of charge on the Web at http://www.jsac.or.jp/analsci/.

References

1. J. M. Berg, J. L. Tymoczko, and L. Stryer, "*Biochemistry*", 7th ed., **2012**, Freeman, New York.
2. G. Ling and R. W. Gerard, *J. Cell. Comp. Physiol.*, **1949**, *34*, 383.
3. A. L. Hodgkin and B. Katz, *J. Physiol.*, **1949**, *108*, 37.
4. M. J. Berridge, *J. Physiol.*, **1988**, *403*, 589.
5. E. Neher and B. Sakmann, *Sci. Am.*, **1992**, *266*, 44.
6. J. R. Wilson, R. B. Clark, U. Banderali, and W. R. Giles, *Channels*, **2011**, *5*, 530.
7. A. Waggoner, *J. Membr. Biol.*, **1979**, *27*, 317.
8. J. Plášek and K. Sigler, *J. Photochem. Photobiol. B*, **1996**, *33*, 101.
9. L. M. Loew, *Pure Appl. Chem.*, **1996**, *68*, 1405.
10. S. Antić and D. Zečević, *J. Neurosci.*, **1995**, *15*, 1392.
11. Y. Momose-Sato, K. Sato, T. Sakai, A. Hirota, K. Matsutani, and K. Kamino, *J. Membrane Biol.*, **1995**, *144*, 167.
12. A. L. Obaid, L. M. Loew, J. P. Wuskell, and B. M. Salzberg, *J. Neurosci. Methods*, **2004**, *134*, 179.
13. Y. Wang, G. Jing, S. Perry, F. Bartoil, and S. Tatic-Lucic, *Opt. Express*, **2009**, *17*, 984.
14. C. Stadele, P. Andras, and W. Stein, *J. Neurosci. Methods*, **2012**, *203*, 78.
15. S. Preuss and W. Stein, *PLOS ONE*, **2013**, *8*, 1.
16. V. Montana, D. L. Farkas, and L. M. Loew, *Biochemistry*, **1989**, *28*, 4536.
17. H. Nagatani, R. A. Iglesias, D. J. Fermín, P. F. Brevet, and H. H. Girault, *J. Phys. Chem. B*, **2000**, *104*, 6869.
18. H. Nagatani, D. J. Fermín, and H. H. Girault, *J. Phys. Chem. B*, **2001**, *105*, 9463.
19. T. Osakai, J. Sawada, and H. Nagatani, *Anal. Bioanal. Chem.*, **2009**, *395*, 1055.
20. T. Osakai, T. Yoshimura, D. Kaneko, H. Nagatani, S. H. Son, Y. Yamagishi, and K. Yamada, *Anal. Bioanal. Chem.*, **2012**, *404*, 785.
21. T. Yoshimura, H. Nagatani, and T. Osakai, *Anal. Bioanal. Chem.*, **2014**, *406*, 3407.
22. M. Moriguchi, H. Nagatani, K. Eda, and T. Osakai, *Bunseki Kagaku*, **2016**, *65*, 71.
23. J. Georges and J. W. Chen, *Colloid Polym. Sci.*, **1986**, *264*, 896.
24. R. A. Mackay, S. A. Myers, and A. Blajter-Toth, *Electroanalysis*, **1996**, *8*, 759.
25. J. Chen, O. Ikeda, and K. Aoki, *J. Electroanal. Chem.*, **2001**, *496*, 88.

26. T. Aoki, E. A. Decker, and D. J. McClements, *Food Hydrocolloids*, **2005**, *19*, 209.
27. L. Q. Hung, *J. Electroanal. Chem.*, **1980**, *115*, 159.
28. L. Q. Hung, *J. Electroanal. Chem.*, **1983**, *149*, 1.
29. T. Kakiuchi, "*Liquid-Liquid Interfaces, Theory and Methods*", ed. A. G. Volkov and D. W. Deamer, **1996**, CRC Press, Boca Raton, FL.
30. J. A. Riddick, W. B. Bunger, and T. K. Sakano (eds.), "*Organic Solvents: Physical Properties and Methods of Purification*", 4th ed., **1986**, Wiley, New York.
31. A. Sabela, V. Mareček, Z. Samec, and R. Fuoco, *Electrochim. Acta*, **1992**, *37*, 231.
32. A. K. Kontturi, K. Kontturi, and Z. Samec, *Acta Chem. Scand.*, **1988**, *42*, 192.
33. T. Osakai, T. Kakutani, Y. Nishiwaki, and M. Senda, *Anal. Sci.*, **1987**, *3*, 499.
34. Z. Samec, D. Homolka, V. Mareček, and L. Kavan, *J. Electroanal. Chem.*, **1983**, *145*, 213.
35. S. J. Rehfeld, *J. Phys. Chem.*, **1967**, *71*, 738.